AN ABSTRACT OF THE THESIS OF

<u>DWIGHT EDWARD BARLOW</u>   for the   <u>Master of Science</u>
          (Name of student)   (Degree)

in <u>Mechanical Engineering</u>   presented on <u>February 4, 1970</u>
          (Major)   (Date)

Title: <u>THE STRESS ANALYSIS OF A TRUCK FRAME BRACKET</u>
                            Redacted for Privacy

Abstract approved: _____
                                    Dr. Hans J. Dahlke

In the construction of a cab-over-engine semi tractor, Freight-
liner Corporation of Portland, Oregon uses brackets to make the con-
nection between the front leaf spring mounts, bumper, front hinges
for the tilt-cab and the longitudinal frame rails. One bracket is used
on each side. The integrity of these brackets is essential to the safe
operation of the truck.

This investigation was undertaken to make an estimate of the
stress levels in some special brackets during the various possible
load combinations which simulate actual operation. This estimate
will be used to justify further more precise measurements of the
stresses in the brackets.

The geometry of the brackets was too complex to use analytical
methods and, also, the prototypes were not available. Quarter scale
photoelastic models were built from laminated sheets of epoxy. This
kind of model enables one to detect flat plate bending as well as

in-plane tension and compression stresses with a reflection polar-iscope. After the critical load combination was determined from these models, a second model was prepared and stress frozen to determine the magnitude and location of the maximum stress occurring in the bracket. Dimensional analysis was used to relate the model properties to the prototype.

The results of this investigation indicated that stress levels higher than the yield strength of the material would occur in the right-hand bracket when braking during a right turn. Strain gages should be applied at the point of maximum stress so that the actual stress in the bracket can be measured for this particular loading condition.

The Stress Analysis of a
Truck Frame Bracket

by

Dwight Edward Barlow

A THESIS

submitted to

Oregon State University

in partial fulfillment of
the requirements for the
degree of

Master of Science

June 1970

APPROVED:

Redacted for Privacy

Associate Professor of Mechanical Engineering
in charge of major

Redacted for Privacy

Head of Department of Mechanical and Nuclear Engineering

Redacted for Privacy

Dean of Graduate School

Date thesis is presented _____ February 4, 1970 _____

Typed by Opal Grossnicklaus for Dwight Edward Barlow

ACKNOWLEDGEMENT

TABLE OF CONTENTS

LIST OF FIGURES

LIST OF TABLES

THE STRESS ANALYSIS OF A TRUCK FRAME BRACKET

INTRODUCTION

In the construction of a cab-over-engine semi tractor, the Freightliner Corporation of Portland, Oregon uses brackets to make the connection between the front spring mounts, bumper, front cab hinges, and the frame rails. The positions of these front frame brackets are shown in Figure 1. There is one on the left and one on the right. They are bolted to the channel iron frame rails. The bumper is bolted across the bumper pads, and the front end of the leaf springs are clamped to the spring mounts. The tilting cab is hinged in front on the cab hinges and secured with latches in the back to keep it from pivoting forward during road operation. The left-hand bracket also serves as a support for the steering gear box. The box is bolted on a raised pad on the left side of the bracket. The integrity of these brackets is essential to the safe operation of the truck.

In the case of a particular experimental truck, the geometry of the machinery in the area of the front frame brackets precluded the use of standard parts. Special parts were fabricated from welded plates of 7039-T6 aluminum. These are shown in Figures 2 and 3.

Some analysis of these brackets must be made, as with any load transmitting structure, to estimate if they are strong enough

Y = Up

Right = X   Z = Rear

Coordinate System

Right-hand
bracket

Left-hand bracket

Y

Z

Frame rail

Cab hinge

Front frame
bracket

Bumper pad

Spring mount

Spring
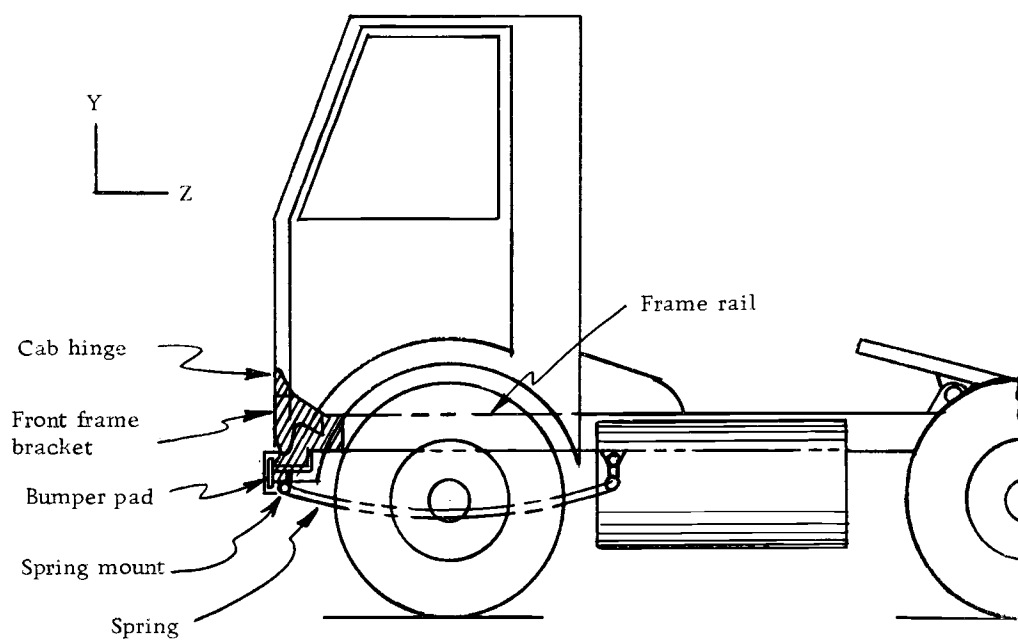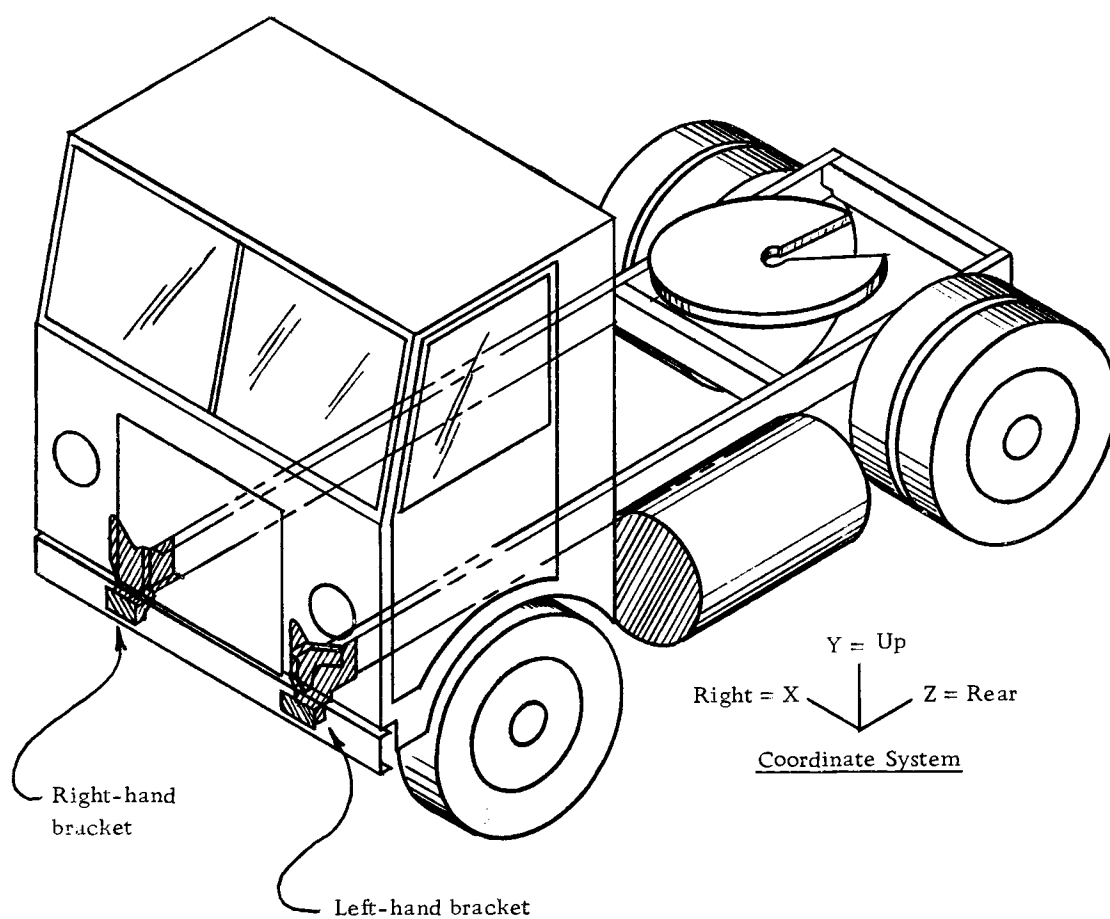
Figure 1.   Location of front frame brackets.

Cab hinge

Frame rail

Bumper
pad

Spring mount

26.0"

19.4"

Fwd.

Fwd.

Left Side View

Right Side View

Figure 2. Right-hand front frame bracket.

Cab hinge

Frame rail

26.0"

Bumper pad

Left Side View

Fwd.

Right Side View
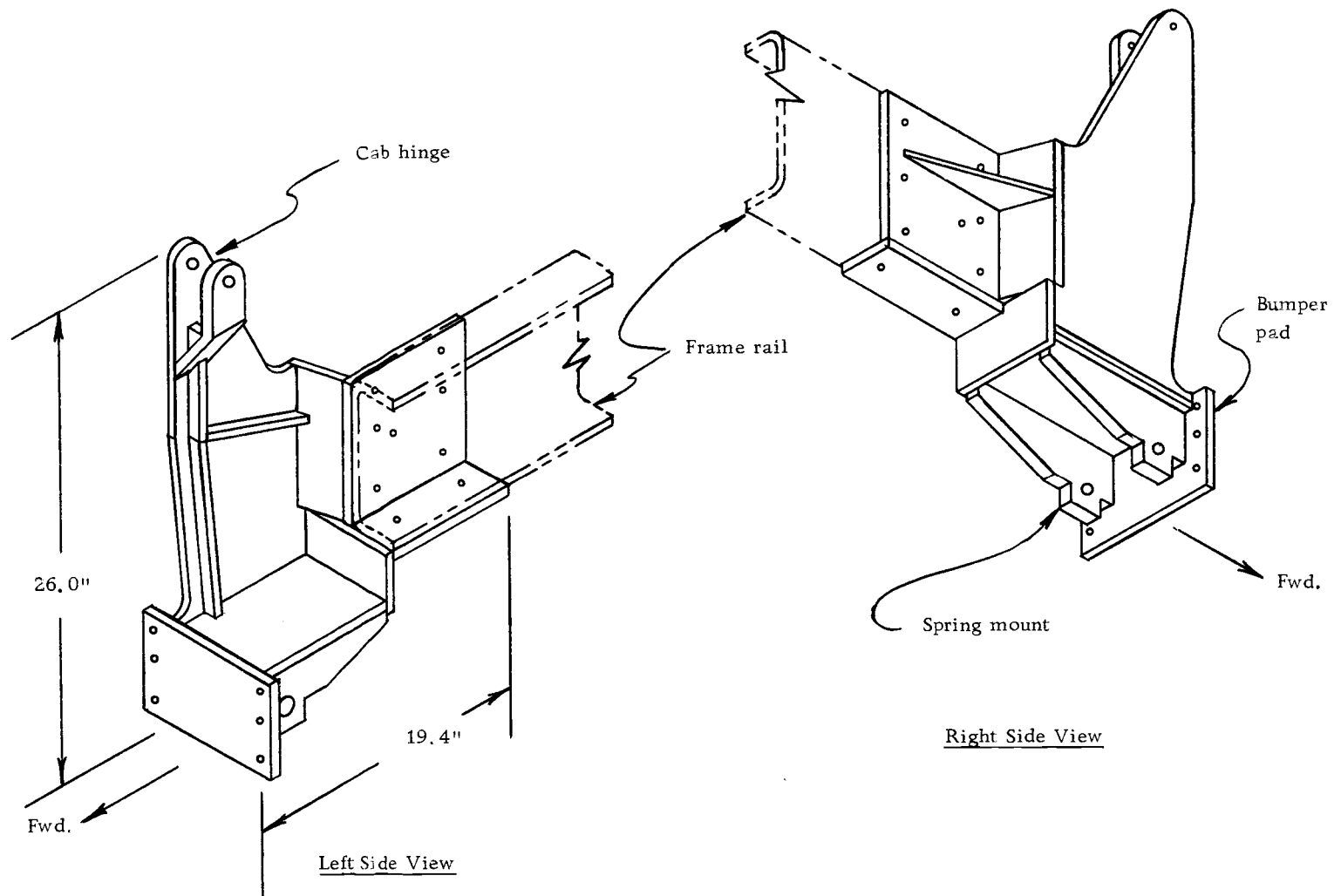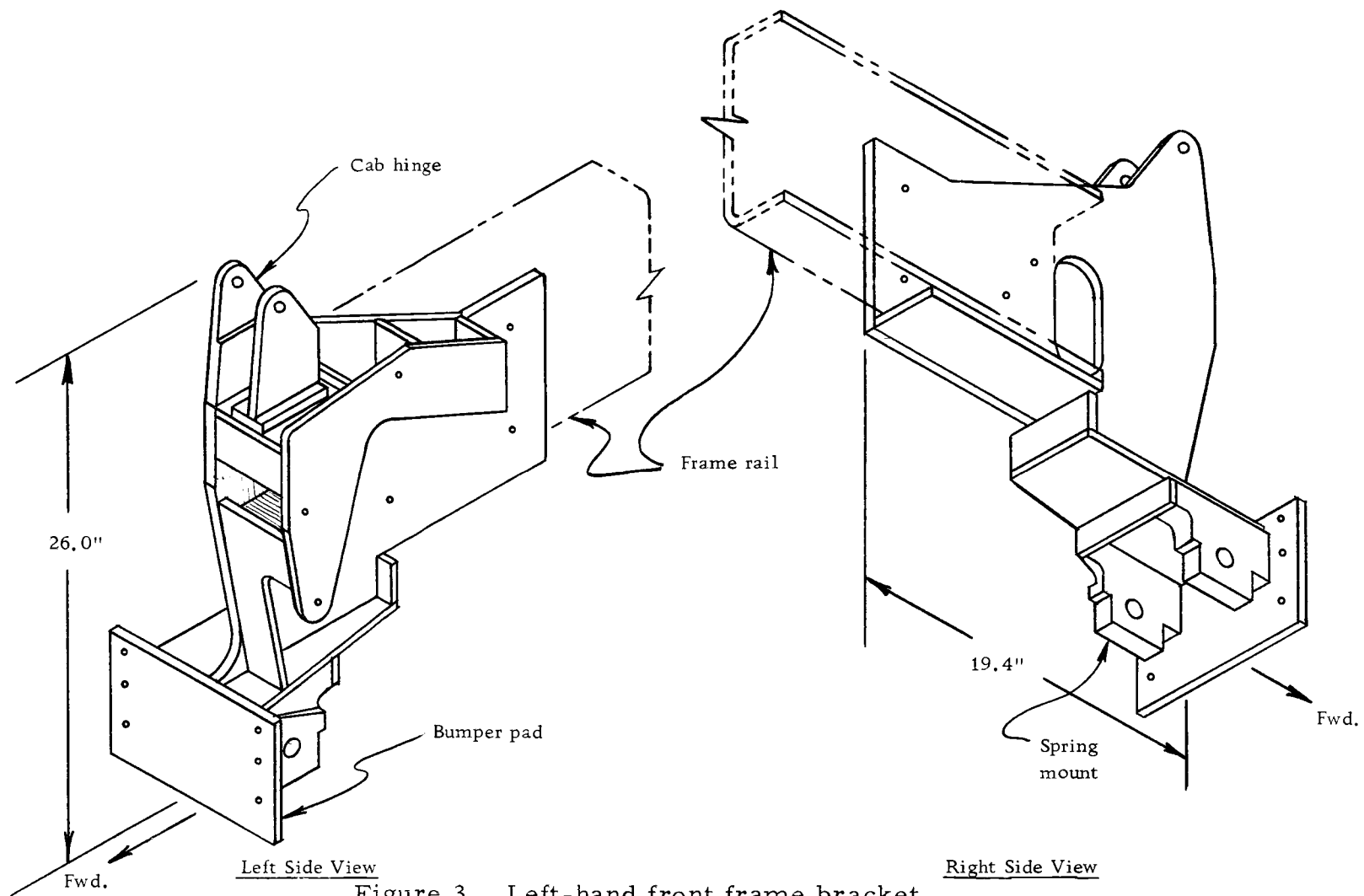
19.4"

Spring
mount

Fwd.

Figure 3.   Left-hand front frame bracket.

4

to function properly. For the preliminary analysis, the designer uses his experience with previous successful parts to design what he feels will be a satisfactory structure. However, if the consequences of a failure are such that they endanger life and extensive property, a more precise analysis becomes necessary.

One can make a fairly accurate estimate of the life expectancy of a part, based on the properties of the material from which it is built, if one can determine the stresses in the part when it is loaded in use. Structures made up of simple geometric shapes can often be handled by analytical methods. But, in the case of complex shapes, such as these front frame brackets, this approach becomes cumbersome and impractical. Even with a digital computer it is not practical to solve this problem analytically. The brackets are three dimensional structures involving bending as well as in-plane tension and compression stresses. This type of problem requires a very large computer and would be costly to solve, if it could be done at all. Thus the analysis must be dispensed with, the part simplified, or other means used. For this case, the first two choices were not desirable and so another approach was selected.

METHODS OF STRESS ANALYSIS

One method of testing a part is to actually use it. If it lasts sufficiently long, it is obviously strong enough. However, if it fails in service, the conditions may be such that it is difficult, or impossible, to determine why it failed. Also, the failure might endanger life and property. Laboratory testing may eliminate the danger of damage and the part may be observed during the test to discover why it breaks.

If the actual parts, or prototypes, are not available or practical to test, one has to use an analogous model. When properly built in relation to its size and material properties, and loaded to scale, it can accurately indicate the stresses that will be encountered in the prototype under similar conditions.

The properties of a model can be related to the prototype by using dimensional analysis (8, 10). For a static elastic model, the following variables need to be considered for the determination of the dimensionless parameters:

E - Modulus of elasticity σ - Stress

μ - Poisson's ratio   P - Load

L - Size δ - Deformation

From these quantities one can derive four independent dimensionless parameters:

$$(\frac{\delta}{L}), \quad (\mu), \quad (\frac{\sigma L^2}{P}), \quad (\frac{P}{E L^2})$$

For similitude to exist between the model and the prototype, each of these parameters for the model must be equal to the corresponding parameter for the prototype.

Two parameters are of major interest:

$$(\frac{\sigma L^2}{P}) \text{ and } (\frac{P}{E L^2})$$

They are used to properly scale the load and stress relative to the model's size and material properties. $(\frac{\delta}{L})$ requires the model's deflections to be proportional to its relative size. This can generally be satisfied by maintaining geometric similarity. (μ) requires Poisson's ratio for the model to be similar to that of the material in the prototype.

STRESS DETERMINATION TECHNIQUES

Various methods are available for measuring the strain and thus the stress in a model. Each one has its advantages and its limitations.

Strain gages can indicate strain quite accurately. They can be used to determine the direction of the principal stresses and they are reusable for any number of tests of the part to which they are applied. They are suitable for measuring the principal strains at a point, but to cover an entire surface with them is very expensive and not a practical approach.

Brittle lacquer or Stress Coat is inexpensive and easy to apply. It is painted on the entire surface of interest and functions because of its low elongation prior to rupture. When the base material is strained, the lacquer cracks at intervals to relieve the relatively excessive strain. The cracks occur perpendicular to the direction of maximum tensile strain and their frequency is a function of the magnitude of the strain. However, this is not a very accurate function and the method is best suited to qualitative analysis. Obtaining information on lines of equal strain requires a lengthy procedure and once a coating is cracked on one test, it must be removed and a new one applied for the next test.

Photoelastic methods can be used (2, 4, 5). In this technique,

a model is made of a transparent birefringent material. That is, the

material behaves such that when it is strained, the index of refrac-

tion along each of the principal strain directions varies as a linear

function of the strain in that direction. If the principal strains are

not equal, then the indices of refraction will not be equal for light

vibrating in the two planes (see Figure 4). When a beam of polarized

light passes through the model, it is divided into two components,

each parallel to a principal strain direction. Due to the different

indices of refraction for each component, they are retarded by differ-

ent distances during their transmission. Thus, there is a phase

difference, α, between the two emerging components whenever the

principal stresses are not equal. This phase difference can be

measured by using an "analyzer" which is actually another polar-

izer. If the analyzer is placed in the path of the beam emerging

from the model, the component of each of the two components enter-

ing the analyzer, which is parallel to the plane of transmission of

the analyzer, will be transmitted. The rest of the beam will be

blocked out. If a monochromatic light source is used, only one

wavelength, λ, is present. Every time the stress is such that the

relative phase difference is $n\lambda$, where n is an integer, the compo-

nents will interfere and no light will be seen by the observer. This

condition is called a "fringe," and will appear as a dark line or area

on the model. All points of the model on the same fringe have the

same difference in principal strains. Any other amount of phase dif-
ference will allow light to be transmitted and will appear as a light
area on the model. The principle of a simple polariscope is shown
in Figure 4.

It should also be noted that if the plane of the polarizer is par-
allel to a principal direction, the light is unaffected by the model.
If the planes of the polarizer and analyzer are 90° different so as to
produce a dark background, a dark line or area appears on the model
at all points where the principal strains are parallel to that direction.
These dark lines are called isoclinics. By rotating the polariscope
relative to the model and noting the location of the isoclinics, the
direction of the principal strains at any point can be found.

If a material which obeys Hooke's law ($\sigma = Ee$) is used, the
strains, and thus the fringes can be related to the difference in prin-
cipal stresses. This can be written as

$$\alpha = n\lambda = ct(\sigma_1 - \sigma_2)$$

where σ_1 and σ_2 are the principal stresses, t is the thickness of the
model, c is a constant which depends on the properties of the par-
ticular material, λ is the wavelength of the light, n is the number
of fringes, or "fringe order," and α is the phase difference between
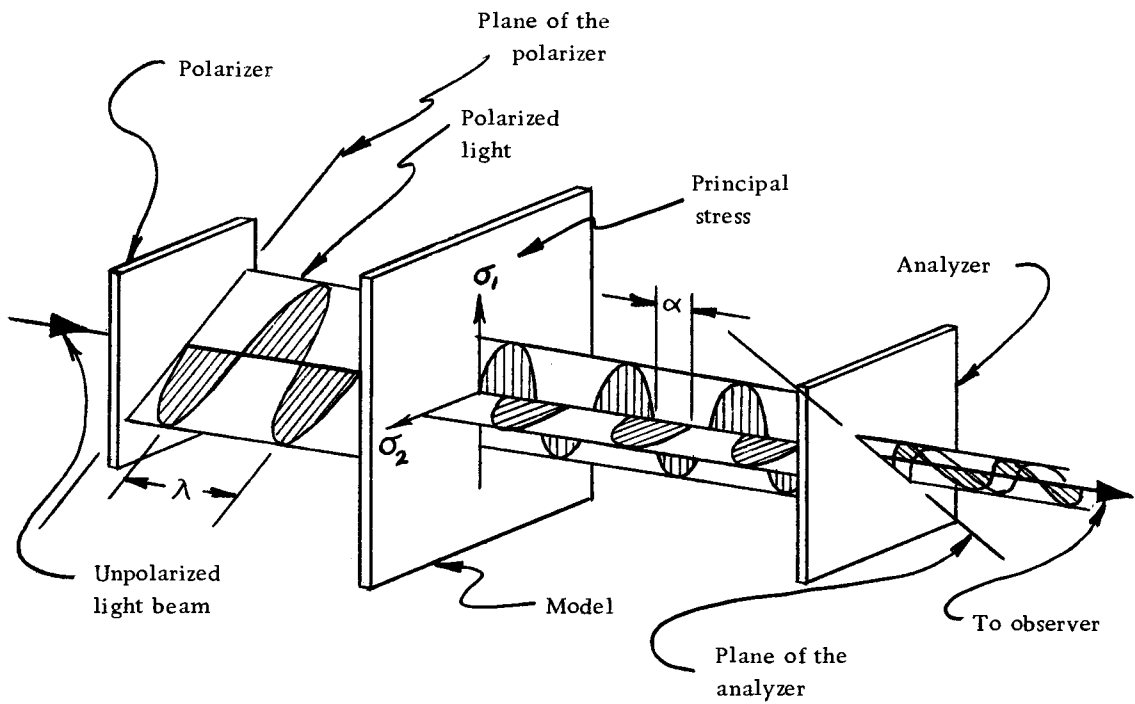the two components of the observed beam. The fringe value of the
material, f, is defined as

Plane of the
polarizer

Polarizer

Polarized
light

Principal
stress

Analyzer

σ_1

σ_2

α

λ

Unpolarized
light beam

Model

Plane of the
analyzer

To observer

Figure 4. Polariscope.

Model

Unpolarized
light source

Polarizer

Reflective
surface

Observer

Analyzer

t
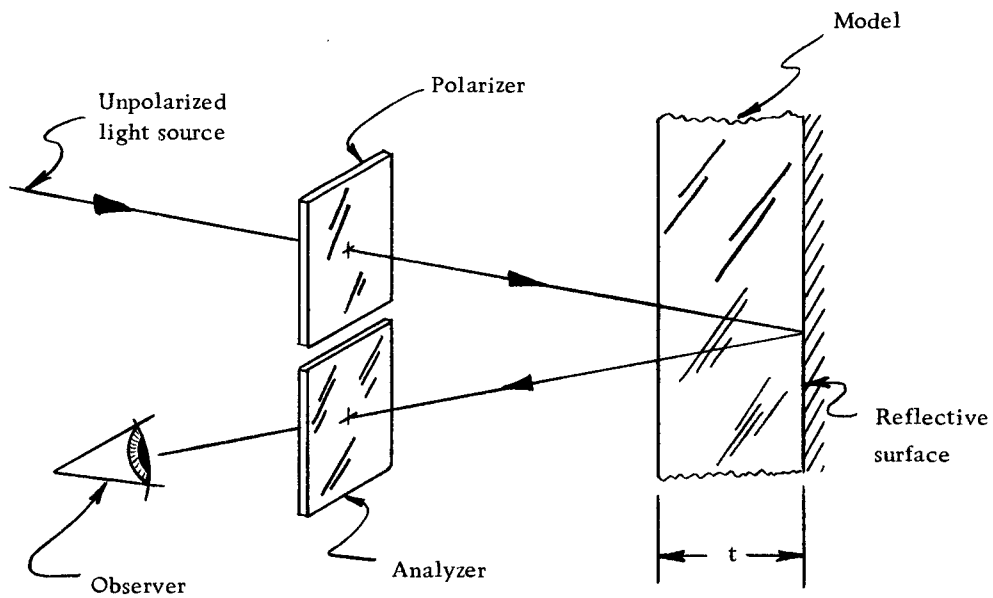
Figure 5. Reflection polariscope.

$$f = \lambda / c = \frac{(\sigma_1 - \sigma_2)t}{n} \frac{psi. - in.}{fringe}$$

This value is a measured property of each material. Using the definition of f, one can express the difference in principal stresses as:

$$\sigma_1 - \sigma_2 = \frac{nf}{t}$$

A special condition exists whenever one principal stress is zero, such as at a free boundary or in a uniaxial stress field. The remaining stress can then be solved for directly. Otherwise, the problem of solving for the magnitudes of the principal stresses is quite complex. One must use either a numerical integration technique called the "shear difference" method, or an experimental technique called the "oblique incidence" method, which determines the sum of the principal stresses and thus provides a second relationship to be used in the determination of the two principal stresses. Often other techniques, such as strain gages, are employed as supplements to eliminate the need to use the more complex photoelastic methods.

Photoelastic methods can be used even when one does not have optical access to both sides of a model. This is done by placing reflective coating on the back side of the photoelastic material. Thus, the light which enters the model is reflected at the back surface, as shown in Figure 5. This has the effect of folding the normal polariscope system in the middle. The effective thickness of the model

becomes 2t.

The reflection technique is used in the photoelastic coating method. Here, a photoelastic layer is sprayed on, or cemented to, the surface of a part which has been coated with a reflective material. The part is then loaded and the stress distribution observed as a function of the fringe pattern. This is a simple and effective method.

The reflection technique is also used in the laminated photoelastic model method. This method is based on the fact that when one looks through a photoelastic plate, the fringe order observed is a function of average stress in the material through which the light passes. As shown in Figure 6, the stress distribution through a section subjected to tension or compression has a net value. In the case of pure bending, half of the thickness is in compression and half is in tension (9). Thus, the net stress for the entire thickness is zero, and no fringes will appear. But, by laminating two sheets together with a reflective layer in the middle, one does not see the second half beyond the midplane. The portion observed with a reflective polariscope has a net stress. This can be observed as fringes and the stress in the section calculated.

In the case of combinations of axial loads and bending, the stress distribution is shifted, as shown in Figure 7. Because of this, a knowledge of the stresses on the opposite side of the reflective midplane is necessary to determine what type of loading exists.
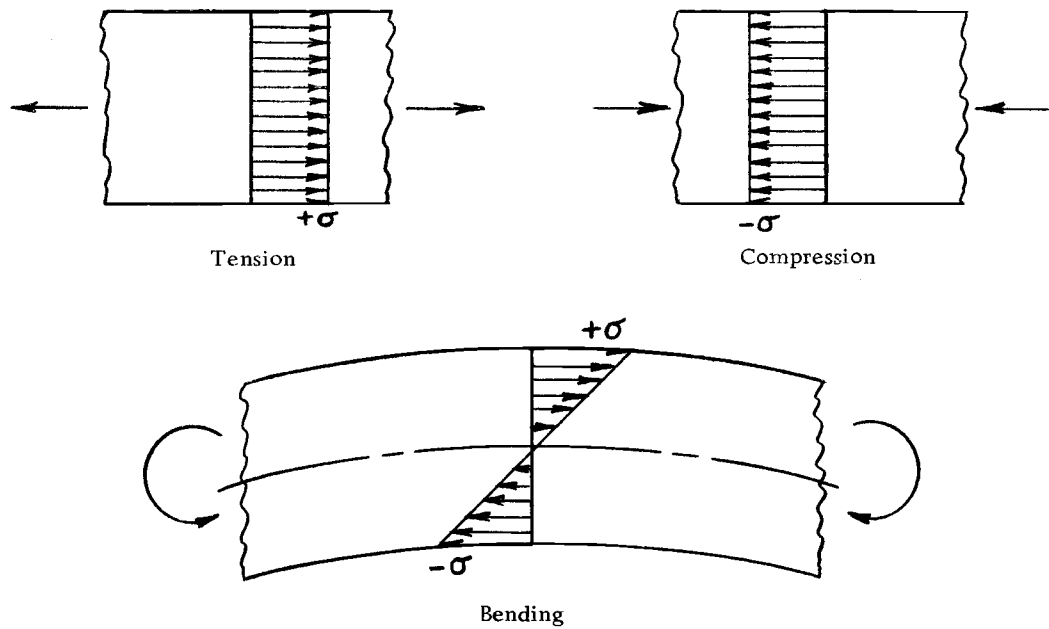
Figure 6. Stress distributions across the thickness of plates with various types of loads.
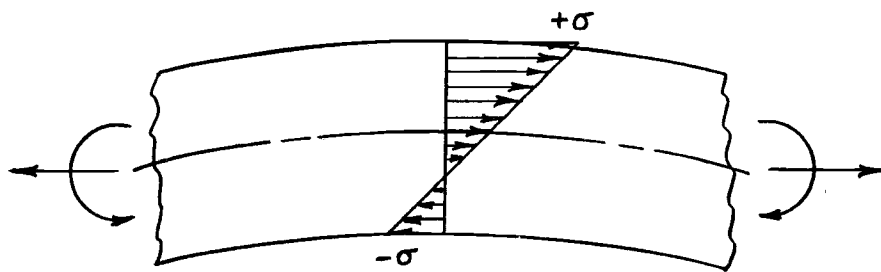

Figure 7. Stress distribution due to combined loading.

Also, because of the lack of a convenient way to optically distinguish tension from compression, a knowledge of the type of loading expected is necessary to complete the analysis.

One way of overcoming the limitations of the laminated method is to look at the edge of the part in question and observe the stress distribution across the thickness. To do this, the part must be sufficiently thin in the direction of observation so that no great change of the stress distribution takes place in its thickness. If a model is not already thin enough when turned edgewise, it must be "stress frozen" and a slice of the proper thickness cut out of the area of interest. This involves heating the loaded model to a temperature where it takes a permanent set, and retains the residual stress pattern. After it is cooled back to room temperature, slices may be cut out of it along various orientations, and the residual stress patterns in those planes observed. In this way, a three dimensional model may be analyzed. One disadvantage of this technique is that the model is destroyed in the process.

ANALYSIS OF THE BRACKETS

This investigation was undertaken for the purpose of making an initial estimate of the maximum stress levels in the brackets. This will be considered with respect to the yield and fatigue strengths of the material and used to establish the advisability of further more precise analyses.

The brackets are subject to a variety of static and dynamic loads, such as the weight of the truck and the turning and braking forces. These are applied in several combinations to account for the various possible operational modes of the truck. The modes considered here are uniform straight ahead driving, braking, turning in each direction and braking while turning in each direction. The stress levels during each of these conditions must be examined.

In order to determine the magnitude of the maximum stress occurring in the brackets, one must first find which load combination produces the maximum stress and where this stress is located on the bracket. After that is done, one must determine the magnitude of the stress to complete the analysis.

Some sort of modeling technique was dictated by the unavailability of the actual brackets. Analytical models were impractical due to the complexity of the geometry. So, an analogous model approach was chosen.

Various methods of analysis were considered. The basic requirements for a method of locating the maximum stress are:

1.   It must be applicable to the entire surface of the part.

2.   It must indicate stress concentrations over and above normally predicted stresses.

3.   It must indicate tension, compression, and bending stresses.

4.   It must be practical considering time and cost.

Strain gages lacked the ability to cover the entire surface in detail. Brittle lacquer is too time consuming to use for the multiple loading conditions, and it is not accurate enough. Stress freezing a photoelastic model is a one-time process not suited to multiple tests when the models are difficult to build. But, a laminated photoelastic model will meet all of the requirements.

The laminated model can be loaded with any combination of loads any number of times with no deterioration of its stress indicating ability. Thus, it is ideally suited to the analysis of a part subjected to a variety of load combinations which consist of tension, compression and bending.

The model making process starts with the casting or purchase of plastic sheets one half the required final thickness. The sheets used in this case were cast from PL-8 epoxy obtained from Photolastic, Inc. of Malvern, Pennsylvania. Two sheets were then

laminated together with cement which creates a light reflecting sur-

face on the midplane of the final sheet. The parts were machined to

shape and assembled with a cement which can be built up like weld

fillets. The procedures outlined in bulletins from Photolastic, Inc.

were followed. The particulars of the process are covered in more

detail in an earlier report to Freightliner Corporation (3).

Quarter scale models were built because the maximum plate

thickness that could be cast was 0.120". This was one eighth the

thickness of the thickest plate required. Two of these sheets cement-

ed together formed a one quarter scale plate.

The requirement for proportional deflections in the model is

satisfied by making it within ±0.010" of the nominal scale dimensions.

Poisson's ratio for the PL-8 epoxy is 0.33 (6). For aluminum,

Poisson's ratio varies between 0.330 and 0.334 (1). Thus, they

are essentially equal and satisfy the requirement for similar

Poisson's ratios.

A right hand coordinate system is used to correlate the orien-

tation of the forces. The X direction is positive toward the right

side of the truck. Y is positive upward and Z is positive toward

the rear of the truck. For convenience of locating the angles on the

models, the directions of the loads are expressed in terms of the

angle of their projections on the X-Y and Y-Z planes. The +Y axis

is used as the datum for the angles. Theta is the angle in the Y-Z

plane measured from the +Y axis toward the +Z axis. Lambda is the angle in the X-Y plane measured from the +Y axis toward the +X axis.

Load data for the brackets was furnished by Freightliner Corporation in the form of the orthogonal components of the maximum spring and cab hinge forces for each loading condition. The conditions considered are static, braking and cornering. The loads are shown in Figure 8. Static forces representing the weight of the vehicle are always present and the other forces are superimposed in the proper combination to simulate braking, cornering in each direction and braking while cornering in each direction. The superposition of the components is tabulated in Tables 1 and 2 for the right and left brackets respectively. They are illustrated acting on the brackets in Figure 9. The static conditions alone produce no significant stresses and thus are omitted from the data tables.

The largest single force was the rearward, or Z component of the braking load on the spring mount. Experimentation indicated that the maximum model load representing this component was 22.5 lbs. Thus, this load was used as a basis for the initial tests of the model. By dividing the actual force of 7200 lbs. by 22.5 lbs., a ratio of 320:1 was established for scaling. The other forces were then divided by 320 and a vector resultant of the sum of the orthogonal components was calculated. The resultants are the forces
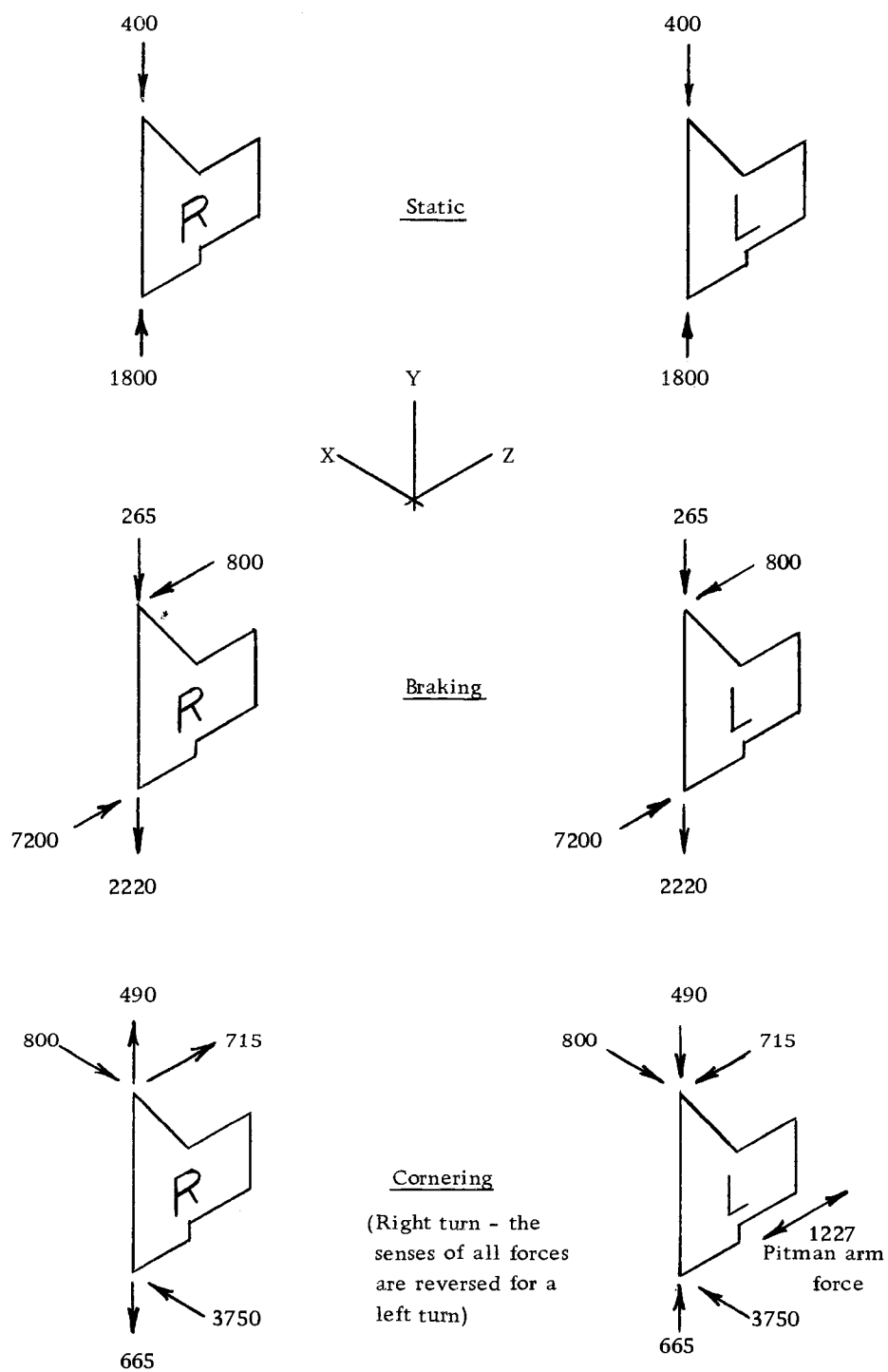
Figure 8.   Bracket forces as supplied by Freightliner.

Table 1. Summation of load components, right-hand bracket.

				Cab			Spring	
			X	Y	Z	X	Y	Z
1.	Static		0	-400	0	0	1800	0
	Brake		0	-265	-800	0	-2220	7200
		Totals	0	-665	-800	0	-420	7200
2.	Static		0	-400	0	0	1800	0
	Rt. turn		-800	490	715	3750	-665	0
		Totals	-800	90	715	3750	1135	0
3.	Static		0	-400	0	0	1800	0
	Left turn		800	-490	-715	-3750	665	0
		Totals	800	-890	-715	-3750	2465	0
4.	Static		0	-400	0	0	1800	0
	Left turn		800	-490	-715	-3750	665	0
	Brake		0	-265	-800	0	-2220	7200
		Totals	800	-1155	-1515	-3750	245	7200
5.	Static		0	-400	0	0	1800	0
	Rt. turn		-800	490	715	3750	-665	0
	Brake		0	-265	-800	0	-2220	7200
		Totals	-800	-175	-85	3750	-1085	7200

Table 2. Summation of load components, left-hand bracket.

|			Cab			Spring		
			X	Y	Z	X	Y	Z
1.	Static		0	-400	0	0	1800	0
	Brake		0	-265	-800	0	-2220	7200
		Totals	0	-665	-800	0	-420	7200
2.	Static		0	-400	0	0	1800	0
	Rt. turn		-800	-490	-715	3750	665	0
		Totals	-800	-890	-715	3750	2465	0
3.	Static		0	-400	0	0	1800	0
	Left turn		800	490	715	-3750	-665	0
		Totals	800	90	715	-3750	1135	0
4.	Static		0	-400	0	0	1800	0
	Left turn		800	490	715	-3750	-665	0
	Brake		0	-265	-800	0	-2220	7200
		Totals	800	-175	-85	-3750	-1085	7200
5.	Static		0	-400	0	0	1800	0
	Rt. turn		-800	-490	-800	3750	665	0
	Brake		0	-265	-800	0	-2220	7200
		Totals	-800	-1155	-1515	3750	245	7200
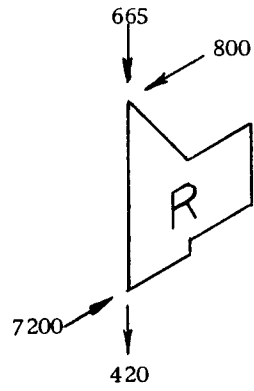
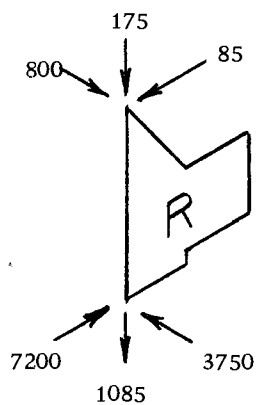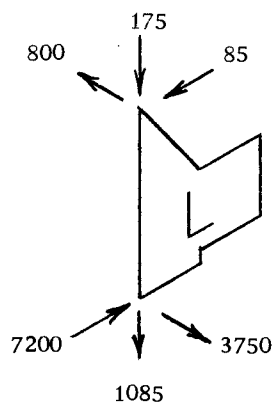1. Brake and static
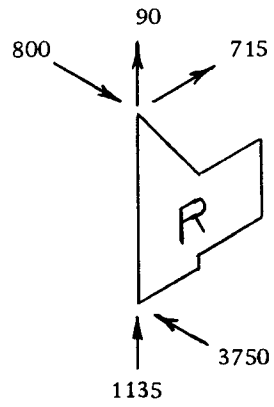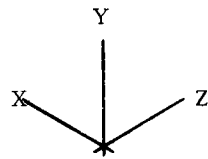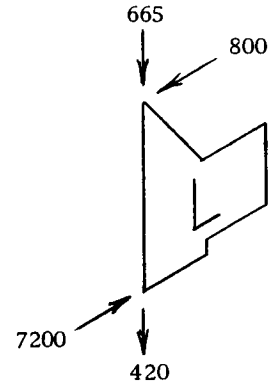
2. Right turn and static
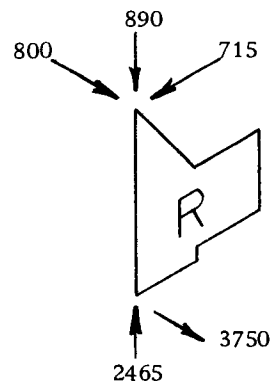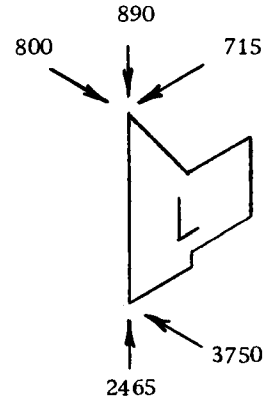
3. Left turn and static
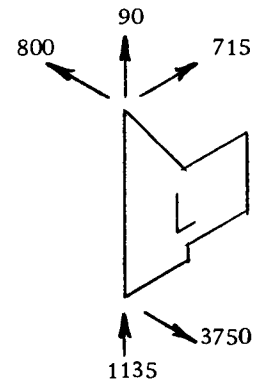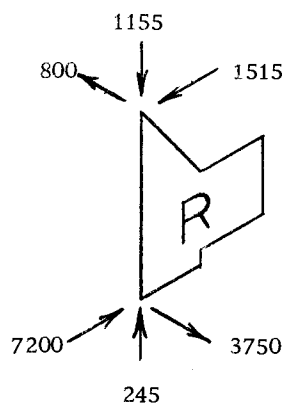
4. Left turn, brake, and static
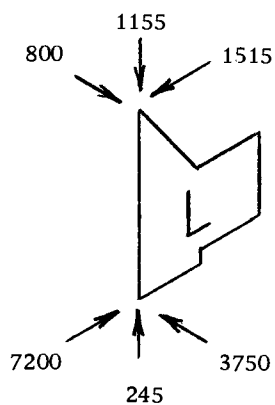
5. Right turn, brake and static

Figure 9. Load components acting on the brackets.

applied to the models. They are listed in Tables 3 and 4 as model loads.

The loads on the brackets can occur at a constant magnitude for at least a short period of time. Therefore, it is reasonable to load the models in a static manner. The model forces were applied by hanging weights so that they were independent of deflections.

The models were bolted to a simulated frame rail and oriented so that the spring loads could be applied by a free hanging weight, as shown in Figure 10. The cab loads were applied by hanging weights on a string over a pulley. The pulley was located so as to give the load a proper direction. Steering loads were applied by using a spring scale. The results were recorded by sketching the fringe pattern as observed through a reflection polariscope.

Generally, the maximum fringe order did not exceed two or three. However, when the brakes were applied during a right turn, an area of high stress was created in the vicinity of the junction of plates 50, 60, 10b, and 10c, on the right-hand bracket. The resulting fringe pattern is shown in Figure 11. The maximum fringe observed is the sixth order fringe at the right front corner of plate 50. This was the highest seen during any of the tests; so, it was chosen for further analysis to determine its magnitude and thus its significance.

Table 3. Applied loads, right-hand bracket.

	Condition		Components X	Y	Z	Directions Θ (°)	Λ (°)	Result-ant	Model loads
1.	Brake,	Cab	0	-665	-800	230	0	1040	3.25
	Static	Spring	0	-420	7200	93	0	7212	22.50
2.	Rt. turn,	Cab	-800	90	715	83	84	1077	3.36
	Static	Spring	3750	1135	0	0	72	3918	12.23
3.	Left turn,	Cab	800	890	-715	219	138	1394	4.36
	Static	Spring	-3750	2465	0	0	303	4488	14.00
4.	Left turn,	Cab	800	-1155	-1515	233	145	2066	6.46
	Brake,	Spring	-3750	245	7200	88	274	8122	25.40
	Static								
5.	Rt. turn,	Cab	-800	-175	-85	206	258	823	2.57
	Brake,	Spring	2750	-1085	7200	99	106	8190	25.60
	Static								

Table 4. Applied loads, left-hand bracket.

Conditions		Components			Θ (°)	Λ (°)	Result-ant	Model loads
		X	Y	Z				
1. Brake,	Cab	0	-665	-800	230	0	1040	3.25
Static	Spring	0	-420	7200	93	0	7212	22.54
2. Rt. turn,	Cab	-800	890	-715	219	222	1394	4.36
Static	Spring	3750	2465	0	0	57	4488	14.00
3. Left turn,	Cab	800	90	715	83	84	1077	3.37
Static	Spring	-3750	1135	0	0	287	3918	12.24
4. Left turn,	Cab	800	-175	-85	206	102	823	2.57
Brake,	Spring	-3750	-1085	7200	99	254	8190	25.60
Static								
5. Rt. turn,	Cab	-800	-1155	-1515	233	215	2066	6.46
Brake	Spring	3750	245	7200	88	86	8122	25.38
Static								

Figure 10.   Left-hand bracket under load.

After the first series of tests, plate 60 was accidently cracked.

A new plate was then machined and placed in the model.   Upon re-

peating the tests the same fringe patterns as before were observed.

Thus, it is reasonable to assume that this stress concentration is a

function of the bracket geometry and not the model construction.

The $\dfrac{P}{E\,L^2}$ parameter was used to calculate the proper scale

model load.   This ratio must be the same for both the model and the

Frame rail

10b

10a

90

10c

50

60

6th order fringe

Y

X

Z

40

30

30

100

Condition = Braking during right turn
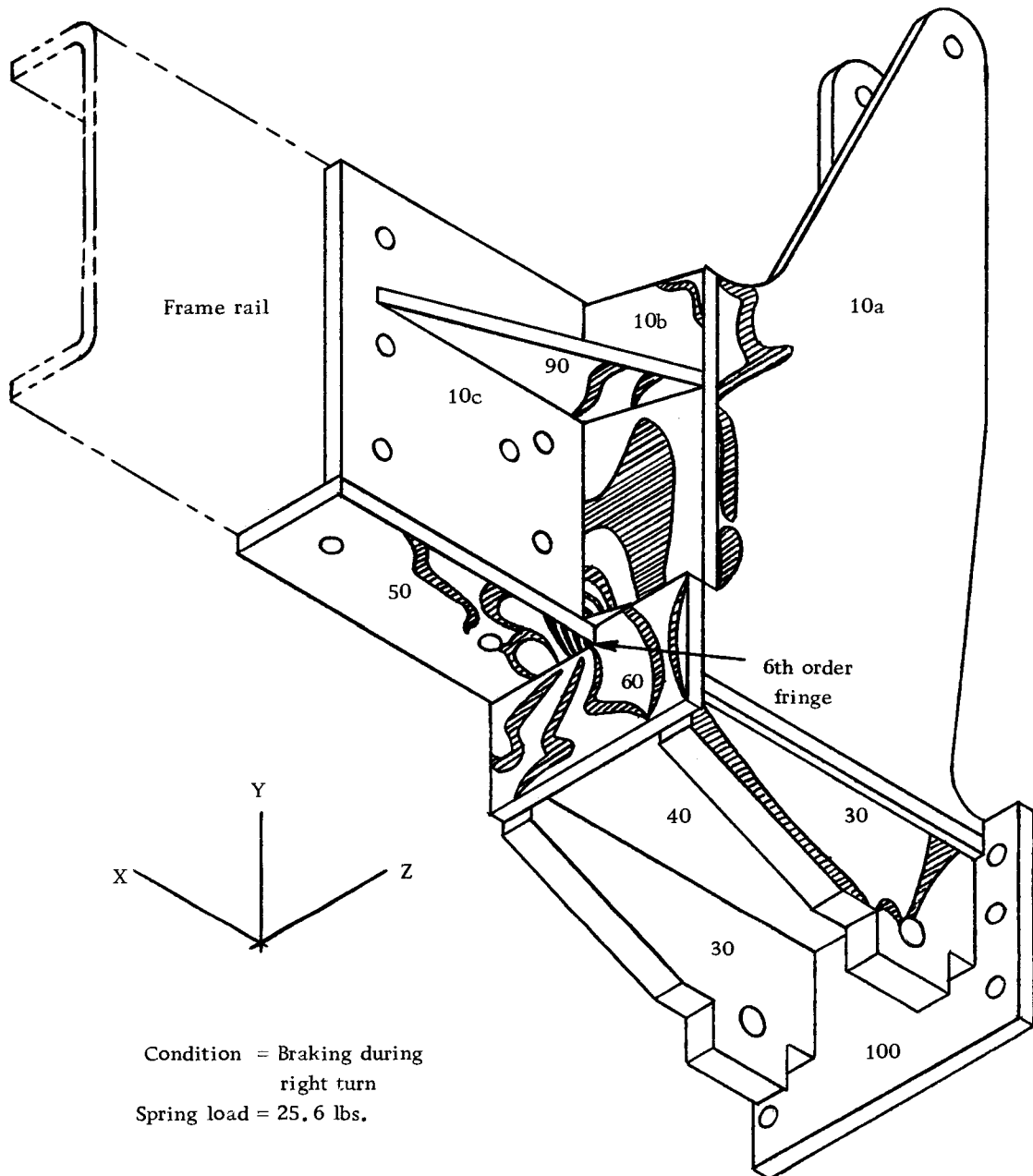
Spring load = 25.6 lbs.

Figure 11. Location of sixth order fringe on right-hand bracket.

prototype. For the right-hand bracket, while braking during a right turn, the resultant spring load, P, equals $(7200^2 + 1085^2 + 3750^2)^{\frac{1}{2}}$ or, 8,190 lbs. E for aluminum is 10×10^6 while E for the Pl-8 epoxy is 0.42×10^6 (7). The model size, L_m, is equal to $\frac{1}{4}L$, where the subscript m is used to denote parameters which apply to the model. Thus:

$$P_m = \frac{P \; E_m L_m^2}{E \; L^2} = \frac{8190 \times 0.42 \times 10^6 \times (\frac{1}{4})^2}{10 \times 10^6 \times 1^2} = 21.5 \text{ lbs.}$$

Applying a 21.5 lb. load to the model resulted in a fifth order fringe as shown in Figure 12. The principal stress, as indicated by the iso-clinic, was found to be parallel to the longitudinal free edge of plate 50.

In order to observe the stress distribution over the thickness of plate 50, a stress freezing model was built and tested. A 10 lb. load was applied, the model heated so that it would take a permanent set, and then allowed to cool. The final deformation was approximately equal to that which was caused by a 21.5 lb. load without heating.

After the stress freezing, a slice was cut out of the model, as shown in Figure 13. It ran through the area of high stress and was parallel to the direction of the principal stress. The slice was 0.109 in. thick.
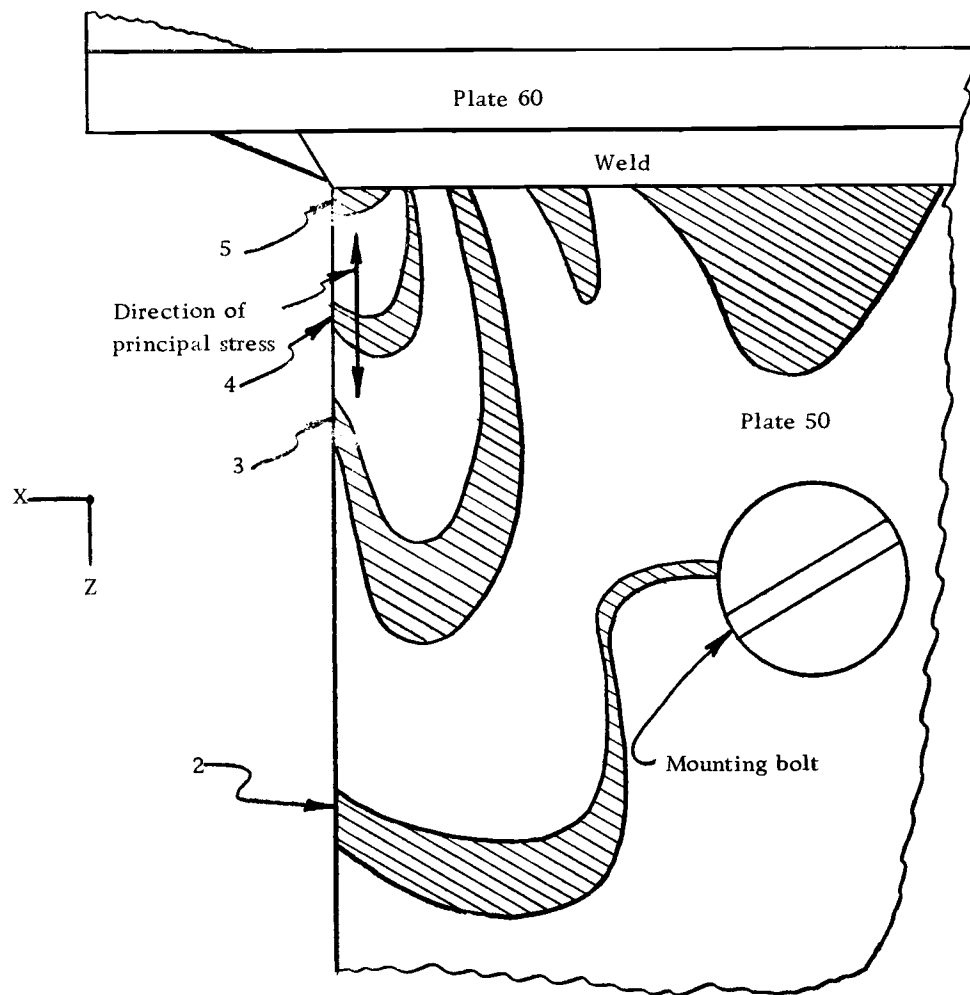
Figure 12. Fringe pattern in Plate 50 due to
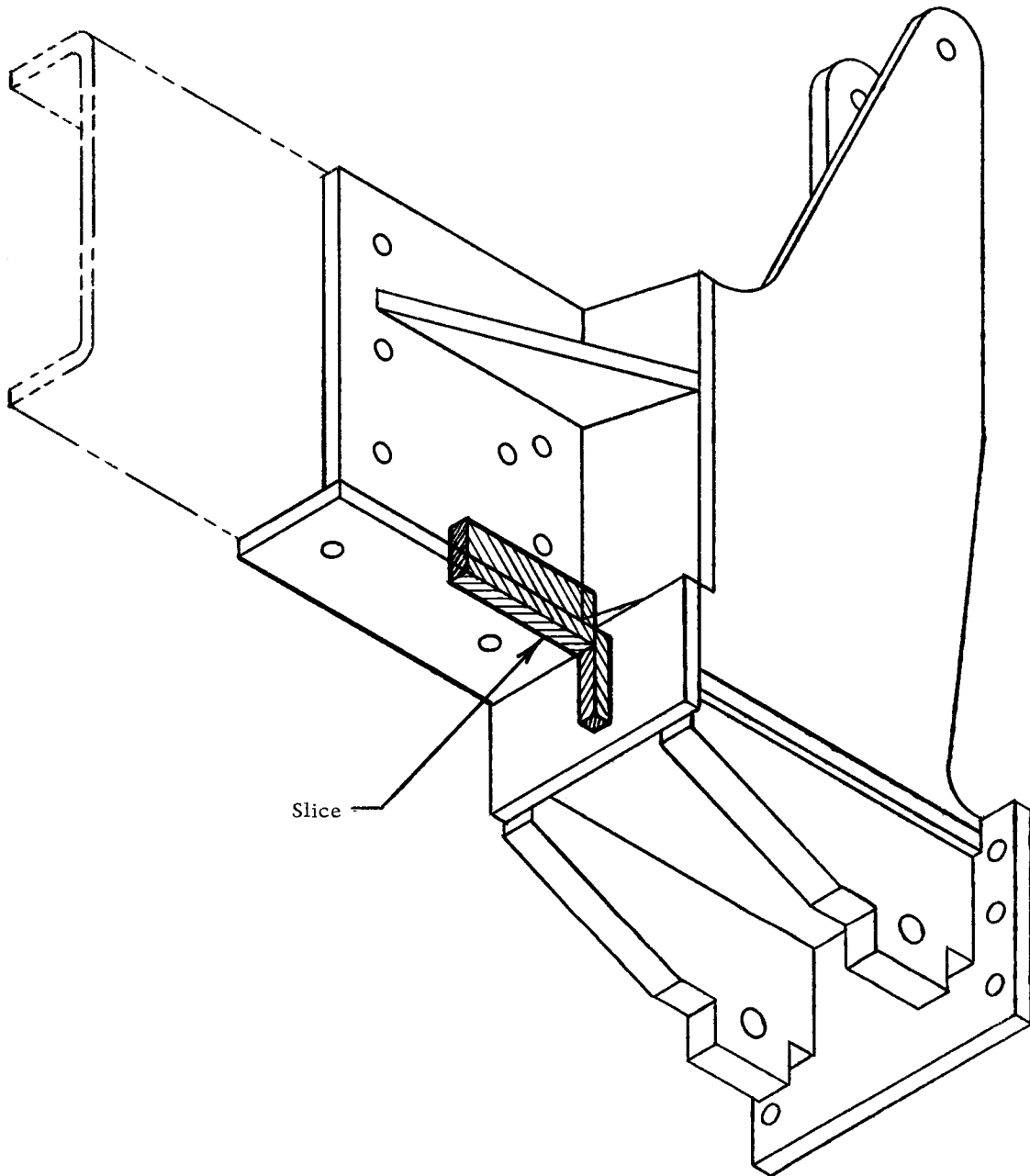21.5 lb. spring load (bottom view).

Slice

Figure 13. Location of slice taken from the
"Stress Freezing" model.

The fringe pattern in the slice, when viewed in the lateral direction, is shown in Figure 14. Section A-A indicates where the fifth order fringe was observed in Figure 12.

Because the fringe order is a function of the average stress in the material through which the light passes, the fifth order fringe seen in Figure 12 represents the average for that section. The maximum is of the most concern. The approximate distribution, based on sec. A-A in Figure 14, is illustrated in Figure 15. This is correlated with the zero fringe order seen when plate 50 is observed from the top side. The maximum is seen to occur at the surface and to be about 4/3 of the average in the lower half of the plate.

The assumption that the same type of stress distribution across section A-A occurs for all loads is based on the fact that the general shape of the fringe pattern, when observed as in Figure 12, does not change with the load. Also, the number of fringes is linear with respect to the load.

The isoclinics indicated that the direction of the principal stress in the slice at section A-A, Figure 14, was parallel to the lower edge of plate 50 and thus lay in the X - Z plane. When viewed from the bottom, as in Figure 12, the isoclinic indicated that the principal stress lay in the Y - Z plane. The only line common to both the X - Z and the Y - Z planes is the longitudinal, or Z axis. Thus, a condition of uniaxial stress must exist at section A-A. This
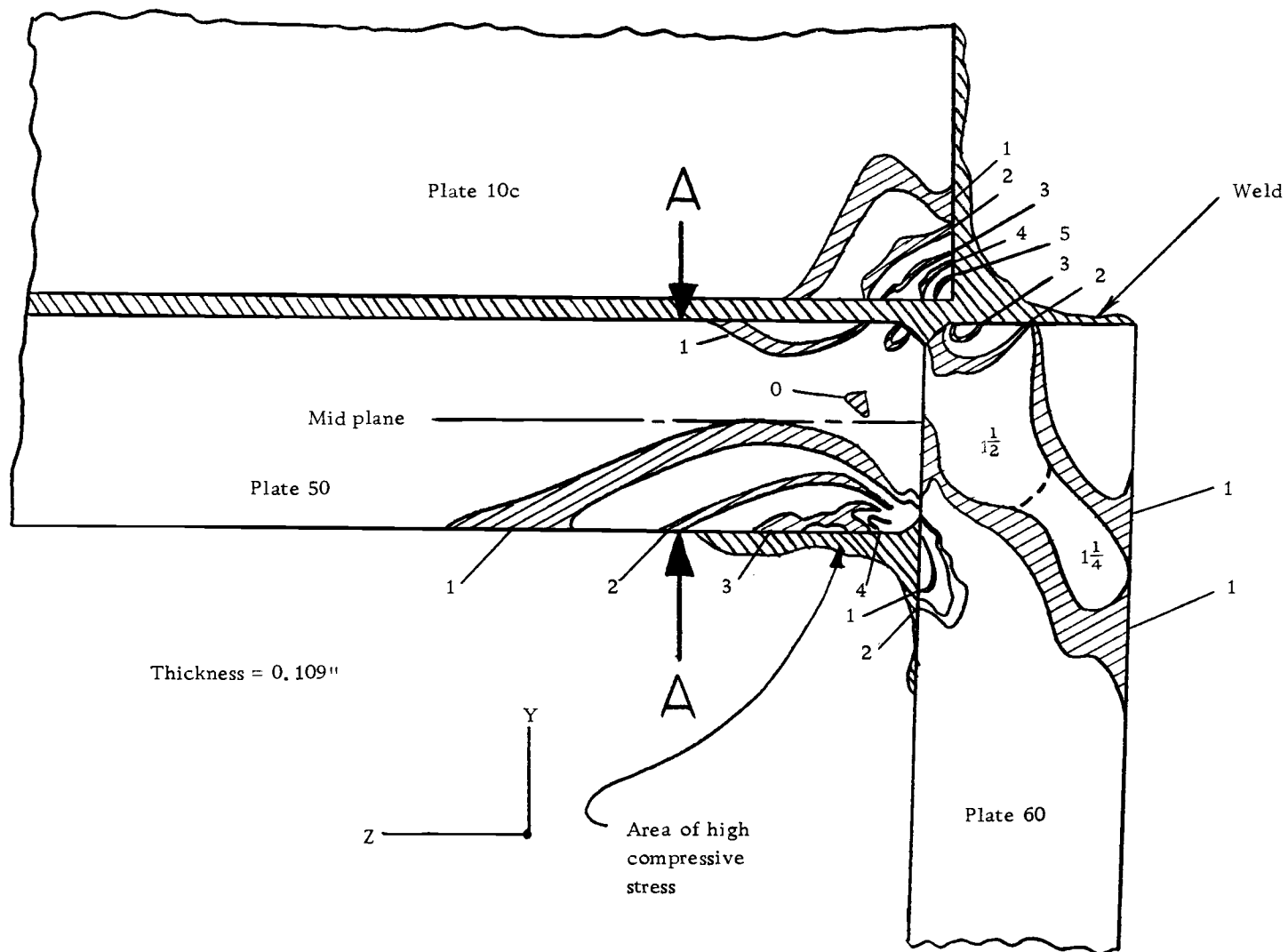
Figure 14.   Fringe pattern in the stress frozen slice.

allows a simplification of the analysis. The fringe order is actually a function of the difference in principal stresses. In this case, all the principal stresses, except the stress in the longitudinal direction, are zero. Thus, the fringe order observed is directly proportional to this one-dimensional stress.

When estimating the stress in the model, the unfrozen model, viewed in the Y direction, is used because it most nearly simulates conditions in the actual bracket. The material stress fringe value, f, relates the number of fringes seen to the stress and section thickness. As determined from tests of the material, f for this model is $83.55 \frac{\text{psi.-in.}}{\text{fringe}}$. The light travels through the epoxy for a distance of twice the distance from the surface to the reflective layer, or, 0.14 in. Using the stress distribution across section A-A, as shown in Figure 15, the fringe value at that section, when viewed in the Y direction, would be 5 x 4/3, or $\frac{20}{3}$ fringes if all of the material was stressed at the same level as the surface material. The surface stress in the model at section A-A is then calculated as follows:

$$\sigma = n\frac{f}{t} = \frac{20}{3} \frac{83.55}{0.14} = 3,980. \text{ psi.}$$

To relate the model stress, σ_m, to the actual bracket stress, the dimensionless parameter $\frac{\sigma L^2}{P}$ is used. The requirement is that:

$$\frac{\sigma L^2}{P} = \frac{\sigma_m L_m^2}{P_m}$$

where the subscript m refers to the model and the lack of a sub-
script refers to the actual bracket.   Solving the equation for σ gives
the following results:

$$\sigma = \sigma_m \frac{L_m^2}{L^2} \frac{P}{P_m} = \sigma_m \frac{(\frac{1}{4})^2}{1} \frac{8190}{21.5} = 23.8\,\sigma_m$$

Substituting the value for σ_m, the stress in the bracket is predicted
to be:

$$\sigma = 23.8\,\sigma_m = 23.8\,(3980) = \underline{94,700}\ \text{psi.}$$

This would certainly be a significant stress if it occurred in a bracket
made of aluminum.

Also, it should be considered that, based on the stress pattern
in Figure 14, there is the possibility of stress of magnitudes 2 to $2\frac{1}{2}$
times this occurring in the areas under the welds.   Unfortunately,
the weld areas themselves are opaque and the magnitude of the stress
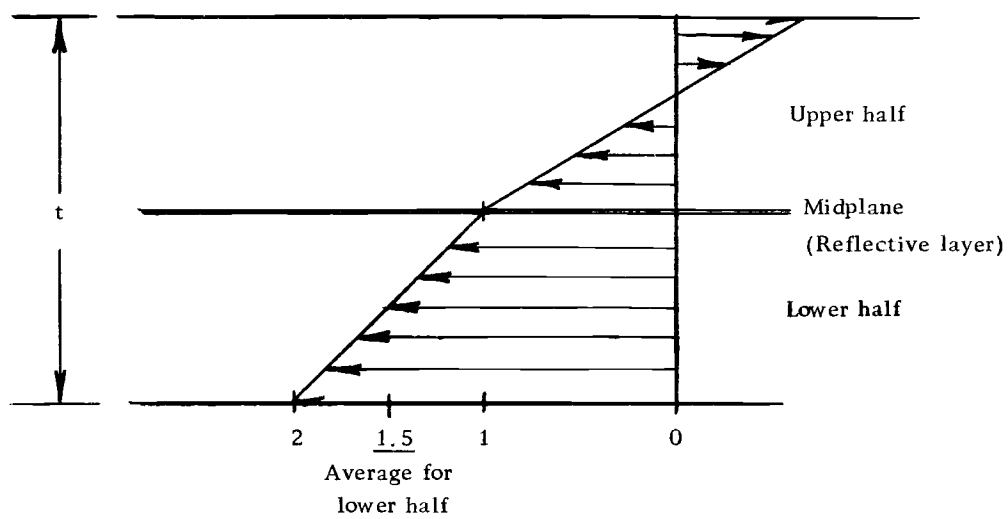in these areas can not be determined from this model analysis.

Figure 15. Stress distribution across Plate 50 at section A-A.

CONCLUSIONS AND RECOMMENDATIONS

The conclusion reached by this analysis is that significantly high stresses will occur in the right-hand bracket when braking during a right turn. The yield strength of the 7039-T6 aluminum is 45,000. psi. Thus, even if there are large errors in this analysis, the stress would still be worthy of consideration. There is the possibility of immediate rupture or at least a definite fatiguing of the metal. In either case, the failure, when it happened, would cause loss of control of the truck and thus a wreck.

It should be noted that this analysis considers only the maximum static loads applied separately to each bracket. Vibration and shock loads due to rough road surfaces are not considered. Loads or restraints due to the interconnection of the brackets through the bumper, which would tend to stop the brackets from twisting about the vertical axis, are also not considered. Twisting of the truck frame would apply unknown loads through the bumper mounting pads along all axes and possibly high moments about the Z axis.

When considering the fact that the brackets have been successfully run on the track without failure, three possibilities exist. First, it is possible that the truck has never been subjected to maximum braking during a maximum right turn. This combination should be an infrequent occurrence. Second, the presence of the bumper with

its bracing effect may be sufficient to prohibit the twisting in the bracket, which is necessary to cause the high stress condition. Third, while failure has not already occurred, it might be imminent due to fatigue. Thus, it would be only a matter of time before failure does occur.

It is recommended that the areas of the junction of plates 50, 60, 10b, and 10c of the right bracket be closely inspected for cracks. Sonic testing or dye penetrant would greatly facilitate the inspection.

If no defects or signs of impending failure are noticed, strain gages should be placed on the lower surface of plate 50 in the right forward corner, as shown in Figure 16. They should be located a distance less than the thickness of plate 10c away from the edge and as close behind the weld fillet as possible. Then readings should be taken while braking during a right turn to check if the actual stress levels are of concern. If they are significant, corrective measures should be taken immediately.

It would also be of interest to take readings of the stress levels in the brackets with the bumper removed. This would confirm or disprove this investigation and establish the validity of the test method as well as the significance of the bumper to the bracket stresses.
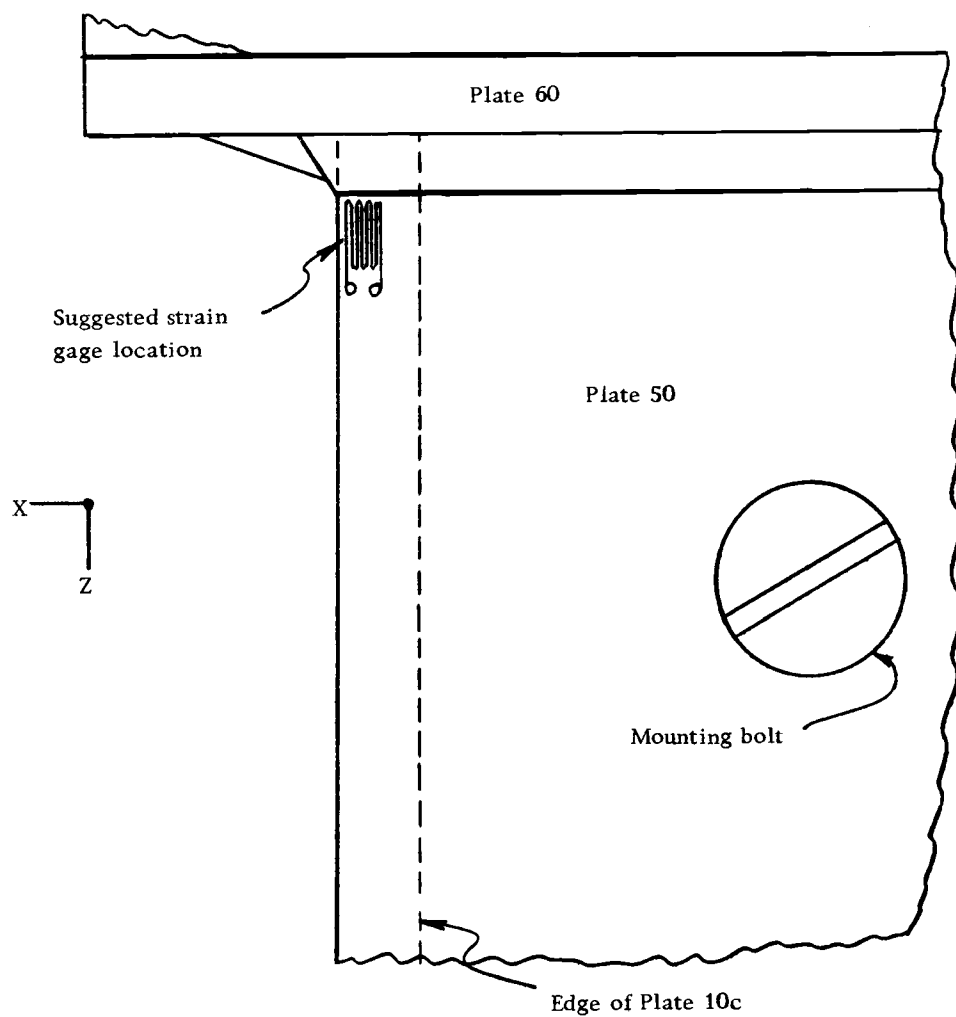
Figure 16.   Suggested location and orientation of a
strain gage.   (Bottom view of bracket.)

BIBLIOGRAPHY

1. Baumeister, T. (ed.). Marks' Standard Handbook for Mechanical Engineers. 7th ed. New York, McGraw-Hill, 1967. Various paging.

2. Crites, N. A., H. Grover and A. Hunter. Experimental Stress Analysis by Photoelastic Techniques. Product Engineering 33: 57-69. Sept. 3, 1962.

3. Dahlke, H. J. and D. E. Barlow. Stress Analysis, Right and Left Front Frame Brackets, P-051-088 and P-051-089. Oregon State University, Corvallis, Ore. Sept. 1969.

4. Durelli, A. J. and W. F. Riley. Introduction to Photomechanics. Englewood Cliffs, Prentice-Hall, 1955. 402 p.

5. Frocht, M. M. Photoelasticity, Vol. 1, New York, Wiley, 1941. 411 p.

6. Photolastic, Inc. Instruction Manual for 030 Series Reflection Polariscope. Malvern, Pa., n.d. 69 p.

7. Photolastic, Inc. Materials for Photoelastic Coatings and Photoelastic Models. Malvern, Pa., n.d. 8 p.

8. Streeter, V. L. Fluid Mechanics. 3d ed. New York, McGraw-Hill, 1962. 555 p.

9. Timoshenko, S. and D. H. Young. Elements of Strength of Materials. 5th ed. Princeton, Van Nostrand, 1968. 377 p.

10. Young, D. F. Basic Principles and Concepts of Model Analysis. Paper presented to Society for Experimental Stress Analysis. Houston, Oct. 16, 1969. 36 p.